ACS OMEGA

Article

Cite This: ACS Omega 2018, 3, 3257−3266

Amide-Functionalized Chalcogen-Bridged Flexible Tetranuclear Rhenacycles: Synthesis, Characterization, Solvent Effect on the Structure, and Guest Binding

Muthuraman Karthikeyan, Buthanapalli Ramakrishna, Sivalingam Vellaiyadevan, Dhanaraj Divya, and Bala. Manimaran*

Department of Chemistry, Pondicherry University, Puducherry 605014, India

Supporting Information

ABSTRACT: The synthesis of flexible rhenium(I)-based amide-functionalized chalcogen-bridged tetranuclear metallacycles of general formula $[\{(CO)_3Re(\mu\text{-}ER)_2Re(CO)_3\}_2(\mu\text{-}L)_2]$ (**1**−**8**) was achieved by treating rhenium carbonyl with dialkyl/diaryl chalcogenide (RE−ER; E = S and Se) in the presence of ditopic flexible or semiflexible pyridyl ligand with amide functionality (L = *N*,*N*′-bis(4-pyridylcarboxamide)-1,2-ethane (bpce) and *N*,*N*′-bis(4-(4-pyridylcarboxamide)phenyl)-methane (bpcpm)). Compounds **1**−**8** were formed by multicomponent self-assembly under one-pot reaction conditions via oxidative addition of dialkyl/diaryl chalcogenide to rhenium carbonyl with pyridyl ligands. The resultant metallacyclophanes were characterized using elemental analyses, infrared, ultraviolet−visible, and NMR spectroscopic techniques. Metallacyclophanes **1**−**3** and **7** were structurally characterized by single-crystal X-ray diffraction methods. The solvent-induced structural change of flexible tetranuclear metallacyclophane **2** was demonstrated by crystallizing **2** in dichloroethane and dimethylformamide. Molecular recognition capabilities of **2** and **7** were studied with few aromatic compounds containing ethereal linkages.

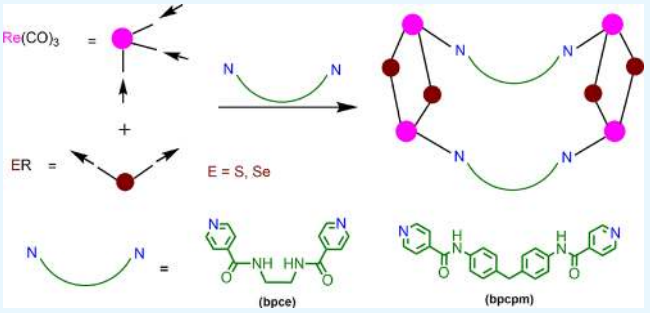

INTRODUCTION

Amide-based compounds are the class of molecules that are important for several chemical disciplines, where the amide functionality forms key linkages in natural and synthetic macromolecules such as proteins, polypeptides, and nylons.[1] Compounds containing amide functional groups are potentially useful in a wide range of industrial applications and possess pharmacological interest.[2] Amide functionality plays a major role in stabilizing various systems through the hydrogen-bond acceptor (C═O group) and hydrogen-bond donor (NH group) and also provides structural flexibility to the systems by facile rotation of functional groups.[3] For instance, cyclic oligoamides show an interesting nanotubular structure and zeolite-like frameworks through intertube NH···O═C hydrogen-bonding interactions.[4] Metal-containing cyclic amides resemble to the cyclic peptide structures. Moreover, the presence of an amide functional group would facilitate the self-assembly process to achieve molecular systems of higher dimensionality via hydrogen-bonding interaction and selective sensing of anions and neutral molecules by providing hydrogen-bonding pockets to the host.[5] Amides serve as binding sites, although they are self-organized to act cooperatively within some convergent molecular architectures.[5d] Thus, the incorporation of organic linkers containing amide functional groups in the formation of the metallacyclic structure is essential and fascinating.

In the literature, only a handful of examples are available pertinent to the tetranuclear metallacyclophanes having amide functionality.[6] By tuning the length and shape of the spacer, a variety of tetranuclear metallacyclophanes have been developed.[7] Mostly, rigid aromatic spacers were employed to prepare these compounds.[7e−i] Rectangular- or bowl-shaped tetranuclear metallacyclophanes were accomplished by changing the bite angle of the donor site.[8] Amide-functionalized tetranuclear metallacyclophanes were probed as hosts for their selective sensing of various anions and macromolecules such as fullerenes, proteins, and so forth, depending on their size and shape.[8,5d] However, reports having amide-containing rhenium metallacyclophanes are hardly available.[9] With this background, we have attempted to synthesize rhenium(I)-based tetranuclear metallacyclophanes containing flexible linkers with amide functionality. In the present study, amide-functionalized ditopic flexible ligands *N*,*N*′-bis(4-pyridylcarboxamide)-1,2-ethane (bpce) and semi-flexible ligand *N*,*N*′-bis(4-(4-pyridylcarboxamide)phenyl)methane (bpcpm) were chosen

Received: January 17, 2018
Accepted: February 12, 2018
Published: March 19, 2018

DOI: 10.1021/acsomega.7b02075
ACS Omega 2018, 3, 3257−3266

Scheme 1. Synthesis of Amide-Functionalized Flexible Tetranuclear Metallacyclophanes 1−8

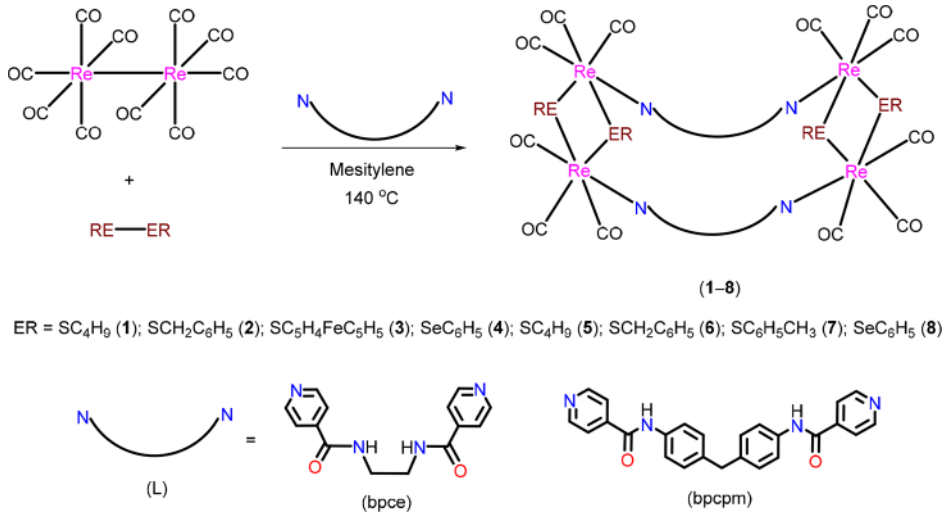

and utilized along with dialkyl/diaryl chalcogenide to react with rhenium carbonyl to form rhenium(I)-based amide-functionalized tetranuclear metallacyclophanes **1**−**8**. Compounds **1**−**8** were characterized using infrared (IR), ultraviolet−visible (UV−vis), and NMR spectroscopic techniques. Some of the metallacyclophanes were structurally characterized by single-crystal X-ray diffraction methods. The adaptive recognition property of **2** was studied by crystallizing the compound in dichloroethane and dimethylformamide (DMF). Molecular recognition capabilities of these metallacyclophanes were analyzed with few aromatic compounds containing ethereal linkages.

RESULTS AND DISCUSSION

The multicomponent heteroligand self-assembly of rhenium carbonyl, dialkyl/diaryl dichalcogenide (RE−ER), and flexible azine ligands with amide functionality (L = bpce and bpcpm) in the mesitylene medium led to the formation of rhenium(I)-based amide-functionalized tetranuclear metallacyclophanes of general formula $[\{(CO)_3Re(\mu\text{-}ER)_2Re(CO)_3\}_2(\mu\text{-bpce})_2]$ (**1**, ER = SC_4H_9; **2**, ER = $SCH_2C_6H_5$; **3**, ER = $SC_5H_4FeC_5H_5$; and **4**, ER = SeC_6H_5) and $[\{(CO)_3Re(\mu\text{-}ER)_2Re(CO)_3\}_2(\mu\text{-bpcpm})_2]$ (**5**, ER = SC_4H_9; **6**, ER = $SCH_2C_6H_5$; **7**, ER = $SC_6H_5CH_3$; and **8**, ER = SeC_6H_5) (Scheme 1). The formation of tetrarhenium compounds **1**−**8** was accomplished by the oxidative addition of dialkyl/diaryl dichalcogenide (RE−ER) to rhenium carbonyl $(CO)_5Re-Re(CO)_5$ in the presence of flexible and semiflexible amide-functionalized pyridyl linkers under facile one-pot reaction conditions. The chalcogenide ligands were coordinated at the equatorial sites of the *fac*-$Re(CO)_3$ core via thiolato/selenolato bridges, whereas flexible ditopic pyridyl linkers were connected at axial sites by Re−N bonds that afforded chalcogen-bridged $M_4E_4L_2$-type rhenacycles.

The resultant metallacyclophanes **1**−**8** were characterized by IR, UV−vis, and ^1H and ^{13}C NMR spectroscopic techniques. The molecular structures were determined for metallacyclophanes **1**−**3** and **7** using single-crystal X-ray diffraction methods. Compounds **1**−**8** were soluble in polar organic solvents and were stable toward air, light, and moisture. Adaptation of solvent-induced diverse geometry of flexible metallacyclophane **2** has been investigated in dichloroethane and DMF. Furthermore, molecular recognition capabilities of **2** and **7** were studied with few aromatic compounds containing ethereal linkages.

IR spectra of compounds **1**−**8** displayed strong bands in the range of ν 2029−1897 cm^{-1} for terminal carbonyl ligands of an octahedrally coordinated *fac*-$Re(CO)_3$ core.[10] The amide C═O stretching frequency of bpce/bpcpm appeared as a weak band at around ν 1605−1681 cm^{-1}. ^1H and ^{13}C NMR spectra of compounds **1**−**8** showed appropriate signals for the bridging ligands, and the spectral data are given in the experimental section. Absorption spectra of **1**−**4** displayed intense bands in the higher energy region λ_{max} 228−311 nm due to ligand-centered transitions and weak bands in the lower energy region λ_{max} 369−383 nm due to metal-to-ligand charge transfer (MLCT) transition, whereas **5**−**8** showed the ligand-centered transitions in the region λ_{max} 226−274 nm as intense bands and the MLCT transitions in the region λ_{max} 305−327 nm as less intense bands.[11]

Good-quality single-crystals of **1**−**3** and **7**, suitable for X-ray diffraction analyses, were obtained by slow evaporation of saturated solution of compound in DMF/dichloroethane at 5 °C. Details about data collection, solution, and refinement are summarized in Tables S1 and S2. The crystal structure of metallacyclophanes **1**−**3** revealed that two $[(CO)_3Re(\mu\text{-}SR)_2Re(CO)_3]$ building blocks were linked by two flexible *N*,*N*′-bis(4-pyridylcarboxamide)-1,2-ethane moieties to afford the tetranuclear metallacyclophane $[\{(CO)_3Re(\mu\text{-}SR)_2Re(CO)_3\}_2(\mu\text{-bpce})_2]$.

In the crystal structure of **1**•DMF, each rhenium center in the *fac*-$Re(CO)_3$ core is coordinated to one nitrogen atom of pyridyl group from the flexible amide-functionalized ligand and two sulfur atoms of butyl sulfide that resulted into a distorted octahedral geometry around it. The molecular structure of **1**•DMF is shown in Figure 1. On the basis of the Re···Re nonbonding distance, the longer and shorter Re···Re distances of **1**•DMF are found to be ∼10.59 and 3.82 Å, respectively. The pyridyl groups in the bpce bridging ligand are arranged in nearly parallel manner because of the weak $\pi\cdots\pi$ interaction with a centroid···centroid distance of 3.512 Å. The amide−amide intramolecular hydrogen-bonding interaction is present between the N(5)−H(5) group and inward O(15) of the bpce ligand at a distance of 2.011 Å.[12] Three outward NH groups of **1**•DMF are having intermolecular hydrogen-bonding interactions with carbonyl oxygen of DMF (N(8)−H(8)···O(19):

DOI: 10.1021/acsomega.7b02075
ACS Omega 2018, 3, 3257−3266

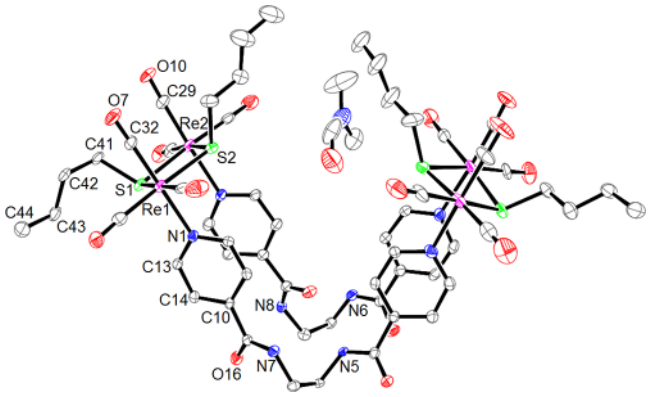

Figure 1. ORTEP diagram of $[\{(CO)_3Re(\mu\text{-}SC_4H_9)_2Re(CO)_3\}_2(\mu\text{-bpce})_2]$ (**1**•DMF) with thermal ellipsoids drawn at 30% probability level. Hydrogen atoms are omitted for clarity. Selected bond lengths (Å) and bond angles (°): Re(1)−N(1) 2.237(8), Re(1)−S(1) 2.501(3), Re(1)−S(2) 2.508(3), Re(1)−C(32) 1.919(11), Re(1)−C(33) 1.929(12), Re(1)−C(34) 1.899(12), N(1)−Re(1)−S(1) 85.3(2), N(1)−Re(1)−S(2) 87.0(2), Re(1)−S(1)−Re(2) 99.3(10), Re(1)−S(2)−Re(2) 99.39(10), S(1)−Re(1)−S(2) 80.79(9), and S(2)−Re(2)−S(1) 80.44(9).

2.054 Å; N(5)−H(5)···O(15): 2.011 Å; and N(7)−H(7)···O(17): 1.950 Å). C−H···π interaction is observed between C(66) of the methyl group of DMF and π cloud of the pyridyl unit in the bpce ligand at a distance of 3.228 Å.[13] These interactions with DMF contribute to the metallacyclophane **1**•DMF to fold up to attain a V-shape structure.

To investigate the solvent-induced adaptive recognition property of **2** under two different solvent conditions, the metallacyclophane $[\{(CO)_3Re(\mu\text{-}SCH_2C_6H_5)Re(CO)_3\}_2(\mu\text{-bpce})_2]$ (**2**) was crystallized in both low and high polar solvents such as dichloroethane and DMF. The molecular structure of **2** crystallized in dichloroethane is shown in Figure 2. Compound **2** crystallized in the monoclinic space group $P2_1/n$ and displayed a rectangular framework. Although a dichloroethane molecule is available in the crystal lattice of **2**, it has been squeezed as it could not be modeled. The dimensions of **2** as defined by Re atoms are ∼17.94 × 3.80 Å.

Intramolecular hydrogen-bonding interaction is observed between the amide NH and oxygen of the carbonyl group projected inside (N(8)−H(8)···O(16): 2.072 Å; N(8)#1−H(8)#1···O(16)#1: 2.072 Å). Intermolecular hydrogen-bonding interaction is observed between the amide NH group projected outside and oxygen of the terminal carbonyl group and oxygen of the amide functional group in the bpce ligand present in the adjacent unit (N(3)−H(3)···O(14) 2.190 Å; N(7)−H(7)···O(16) 2.031 Å).

The molecular structure of **2**•DMF is shown in Figure 3. **2**•DMF displayed a V-shaped structure, and on the basis of the

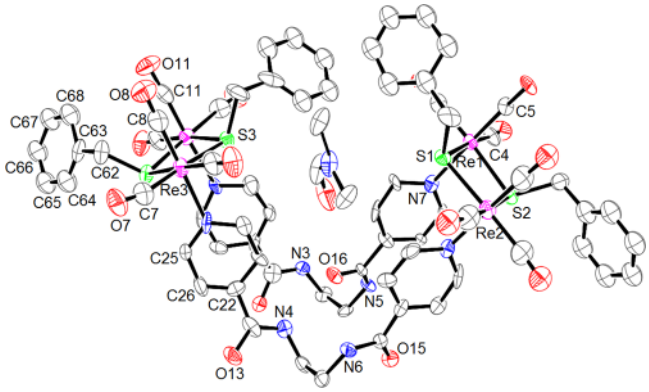

Figure 3. ORTEP diagram of $[\{(CO)_3Re(\mu\text{-}SCH_2C_6H_5)_2Re(CO)_3\}_2(\mu\text{-bpce})_2]$ (**2**•DMF) with thermal ellipsoids drawn at 30% probability level. Hydrogen atoms are omitted for clarity. Selected bond lengths (Å) and bond angles (°): Re(1)−N(7) 2.221(12), Re(1)−S(1) 2.507(4), Re(1)−S(2) 2.508(5), Re(1)−C(4) 1.939(18), Re(1)−C(5) 1.939(5), Re(1)−C(6) 1.89(2), N(7)−Re(1)−S(1) 82.3(3), N(7)−Re(1)−S(2) 84.1(4), Re(2)−S(1)−Re(1) 99.70(13), Re(2)−S(2)−Re(1) 99.59(4), S(1)−Re(1)−S(2) 80.09(14), and S(1)−Re(2)−S(2) 80.16(14).

Re···Re nonbonding distance, the longer and shorter Re···Re distances of **2**•DMF are found to be ∼10.94 and 3.80 Å, respectively. The intramolecular hydrogen-bonding interaction (N(4)−H(4)···O(16): 2.038 Å) is observed between N(4)−H(4) of an amide group and O(16) of another amide group. DMF is occupied as a guest molecule inside the cavity through hydrogen-bonding interaction. Intermolecular hydrogen-bonding interaction is observed between the outward amide NH group and carbonyl group of DMF (N(5)−H(5)···O(17): 1.988 Å). The molecular dimension and hydrogen-bonding interactions of **2**•DMF are comparable to the molecular structure of **1**•DMF.

The crystal structure of $[\{(CO)_3(\mu\text{-}SC_5H_4FeC_5H_5)_2Re(CO)_3\}_2(\mu\text{-bpce})_2]$ (**3**) showed a rectangular framework where each rhenium in the *fac*-$Re(CO)_3$ core is coordinated to one nitrogen atom from the flexible amide-containing pyridyl ligand and two sulfur atoms from the ferrocene sulfide moiety,

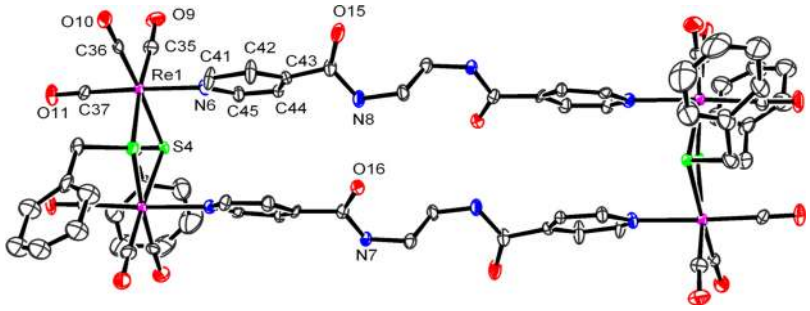

Figure 2. ORTEP diagram of $[\{(CO)_3Re(\mu\text{-}SCH_2C_6H_5)_2Re(CO)_3\}_2(\mu\text{-bpce})_2]$ (**2**) with thermal ellipsoids drawn at 30% probability level. Hydrogen atoms are omitted for clarity. Selected bond lengths (Å) and bond angles (°): Re(1)−N(6) 2.253(10), Re(1)−S(3) 2.504(4), Re(2)−S(4) 2.502(4), Re(1)−C(35) 1.896(14), Re(1)−C(36) 1.924(14), Re(1)−C(37) 1.925(14), N(6)−Re(1)−S(3) 80.16(11), N(6)−Re(1)−S(4) 86.9(3), Re(1)−S(3)−Re(2) 98.79(13), Re(1)−S(4)−Re(2) 98.60(12), S(4)−Re(1)−S(3) 80.16(11), and S(3)−Re(2)−S(4) 79.97(11).

DOI: 10.1021/acsomega.7b02075
ACS Omega 2018, 3, 3257−3266

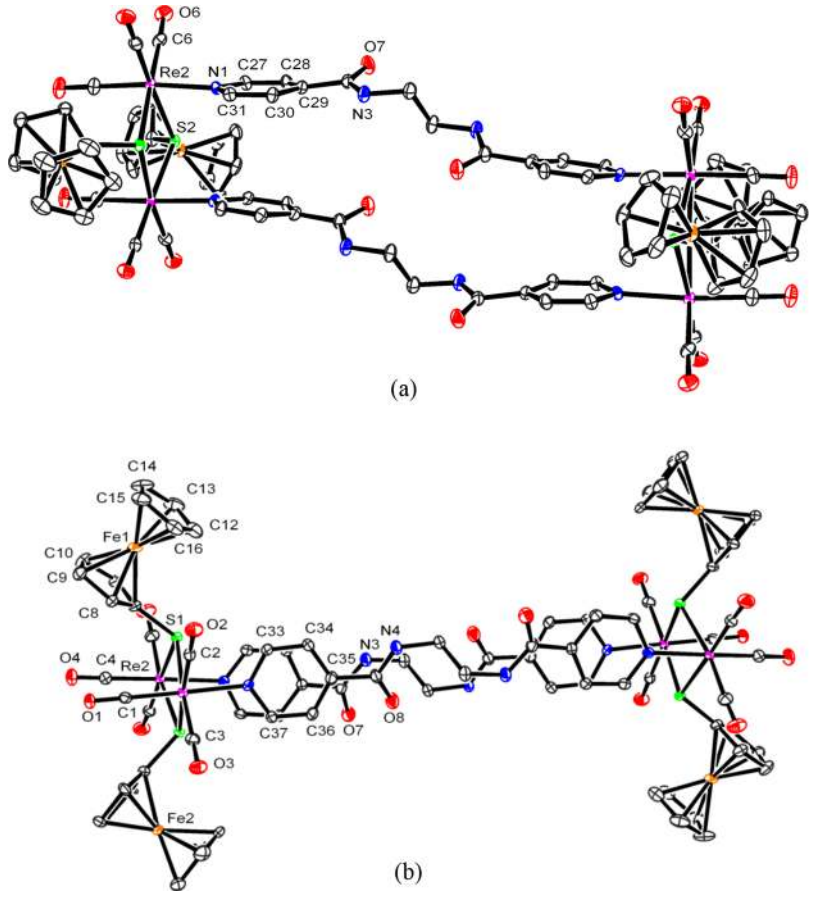

Figure 4. (a) ORTEP diagram of $[\{(CO)_3Re(\mu\text{-}SC_5H_4FeC_5H_5)_2Re(CO)_3\}_2(\mu\text{-bpce})_2]$ (**3**) with thermal ellipsoids drawn at 30% probability level. Hydrogen atoms are omitted for clarity. (b) Top view of **3**. Selected bond lengths (Å) and bond angles (°): Re(1)−N(2) 2.218(6), Re(1)−S(1) 2.504(17), Re(1)−S(2) 2.493(17), Re(1)−C(1) 1.909(8), Re(1)−C(2) 1.917(8), Re(1)−C(3) 1.922(8), N(2)−Re(1)−S(1) 81.66(15), N(2)−Re(1)−S(2) 85.15(15), Re(1)−S(1)−Re(2) 98.32(6), Re(1)−S(2)−Re(2) 98.88(6), S(2)−Re(1)−S(1) 80.60(6), and S(2)−Re(2)−S(2) 80.16(6).

resulting into a distorted octahedral geometry around the metal center. On the basis of the Re···Re distance, the dimensions of **3** are found to be ∼17.91 and 3.79 Å. The molecular structure of **3** is shown in Figure 4. All of the four NHs of the bpce ligand have intermolecular hydrogen-bonding interaction with the carbonyl oxygen of DMF (N(4)−H(4)···O(10) 2.149 Å; N(3)−H(3)···O(9) 2.018 Å; N(4)#1−H(4)···O(10)#1 2.149 Å; N(3)#1−H(3)#1···O(9)#1 2.018 Å). Another hydrogen-bonding interaction is also observed between the C(45)−H(45C) of the methyl group in DMF and O(2) of the oxygen atom in the terminal carbonyl group attached with the rhenium metal center (Figure 5). The CH···π interaction is noticed between the C(9)−H(9) of the cyclopentadienyl moiety of the ferrocenyl group and Cp (centroid) of the ferrocenyl group in the adjacent neighboring unit at a distance of 2.891 Å (Figure 6). Another CH···π interaction is also perceived between C(44)−H(44) of the aldehydic group in DMF and Cp (centroid) of the ferrocenyl group at a distance of 2.925 Å.

The crystal structure of **7**•DMF displayed that the two units of $(CO)_3Re(\mu\text{-}SC_6H_5CH_3)_2Re(CO)_3$ building blocks are linked by two *N*,*N*′-bis(4-(4-pyridylcarboxamide)phenyl)-methane ligands to furnish a tetranuclear hammock-shaped metallacyclophane. Each rhenium in the *fac*-$Re(CO)_3$ core is coordinated to one nitrogen atom of pyridyl group from the amide-containing bpcpm ligand and two sulfur atoms from the *p*-tolylsulfide moiety, resulting into a distorted octahedral geometry around the metal center. On the basis of the Re···Re non-bonding distance, the longer and shorter Re···Re distances of **7**•DMF are found to be ∼22.68 and 3.80 Å, respectively. The Oak Ridge thermal ellipsoid plot (ORTEP) diagram of **7** is shown in Figure 7. The pyridyl groups in the bpcpm ligand are arranged in a parallel fashion with weak $\pi\cdots\pi$ interaction having a centroid···centroid distance of 3.792 Å.[14] Intramolecular CH···π interaction is observed between the CH of the phenyl group and π cloud of the phenyl group of the bpcpm bridging ligand (CH(55)···π(centroid): 2.978 Å; CH(56)···π(centroid): 3.222 Å; CH(27)···π(centroid): 3.642 Å; CH(28)···π-(centroid): 3.172 Å). All of the four NH groups of the bpcpm ligand are involved in the intermolecular hydrogen-bonding interaction with the carbonyl oxygen of DMF (NH(7)···O(17): 1.951 Å; NH(2)···O(18): 2.066 Å; NH(6)···O(20): 2.107 Å; NH(3)···O(19): 2.043 Å) (Figure 8).

A variety of NH···OC interactions have been observed in the molecular structure of the metallacyclophanes **1**, **2**, and **7** with DMF. Especially **1** and **2** adapted to a V-shaped structure upon interaction with encapsulated DMF. These observations encouraged us to study the molecular recognition capability of the metallacyclophanes quantitatively with aromatic compounds containing ethereal linkages. For the host−guest interaction studies, metallacyclophanes **2** and **7** were chosen as hosts owing to their better solubility. 1,3,5-Trimethoxybenzene, 2,4,5-trimethoxybenzaldehyde, and 3,4,5-trimethoxybenzalde-

DOI: 10.1021/acsomega.7b02075
ACS Omega 2018, 3, 3257−3266

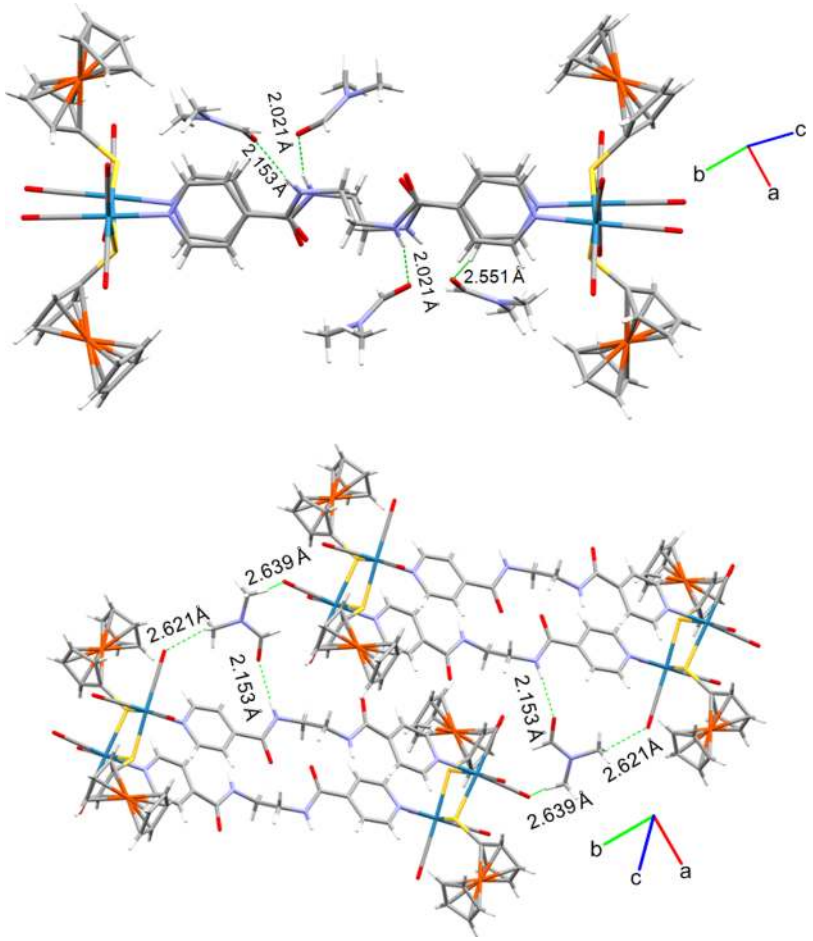

Figure 5. Packing diagrams of **3** showing NH···OC hydrogen-bonding interactions.

hyde were selected as guest molecules. UV−visible absorption and emission spectrophotometric methods were employed to evaluate the binding ability of hosts **2** and **7**, and the experimental details are given in the Supporting Information. During the spectral titration experiments, the concentration of the guest species was kept constant, whereas the concentration of the host was gradually increased. The absorption pattern of the guest was found to enhance with incremental addition of the host that might presumably be due to the formation of the host−guest complex in the ground state. Linear regression has been carried out using the change in the absorption intensity of the guest on *Y*-axis and the change in the concentration of the host on *X*-axis, and the resultant graph showed a good linear correlation. The binding constant was calculated from the slope and intercept obtained from the Benesi−Hildebrand double reciprocal plot.[15] Overlay absorption spectra of the host in the presence of various guests along with the linear regression plot are given in the Supporting Information. In the emission spectroscopic method, the emission intensity of the guest was quenched with an increase in the concentration of the host that might be accounted for the non-luminescent host−guest complex formation in the excited state. Quenching constant was evaluated using the Stern−Volmer equation obtained from the plot of I_0/I and the concentration of the host,[16] where I and I_0 are the fluorescent intensity of the guest in the presence and absence of the host. Overlay emission spectra of the host in the presence of various guests along with the Stern−Volmer plot are given in the Supporting Information. The binding and quenching constants are given in Table 1.

These results showed an efficient host−guest interaction between the metallacyclophanes and guest molecules. The host−guest binding interaction is attributed to the NH···O hydrogen-bonding interaction between the metallacyclophane and aromatic compound. In addition, other supramolecular interactions such as CH···π and π···π interactions may also contribute significantly.

CONCLUSIONS

In conclusion, we have accomplished a facile synthesis of amide-functionalized flexible tetranuclear metallacyclophanes of varying molecular dimensions. The rhenium(I)-based tetranuclear metallacyclophanes were obtained in one-pot reaction condition via an orthogonal-bonding approach. The compounds were characterized by IR, UV−vis, and ^{1}H and ^{13}C NMR spectroscopic techniques. Molecular structures of few metallacyclophanes were ascertained by single-crystal X-ray diffraction methods. The adaptive recognition property of the flexible tetranuclear metallacyclophanes was investigated by crystallizing compound **2** in dichloroethane and DMF. The molecular recognition capabilities of metallacyclophanes **2** and **7** were studied with few aromatic compounds containing ethereal linkages.

DOI: 10.1021/acsomega.7b02075
ACS Omega 2018, 3, 3257−3266

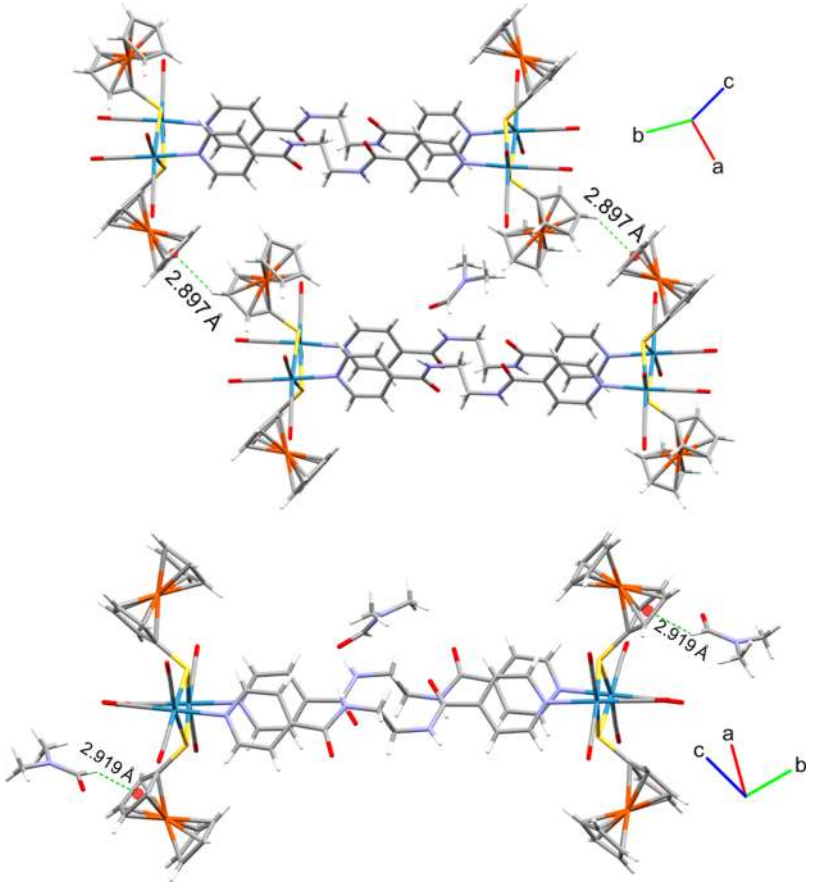

Figure 6. Packing diagrams of **3** showing C−H···π interactions.

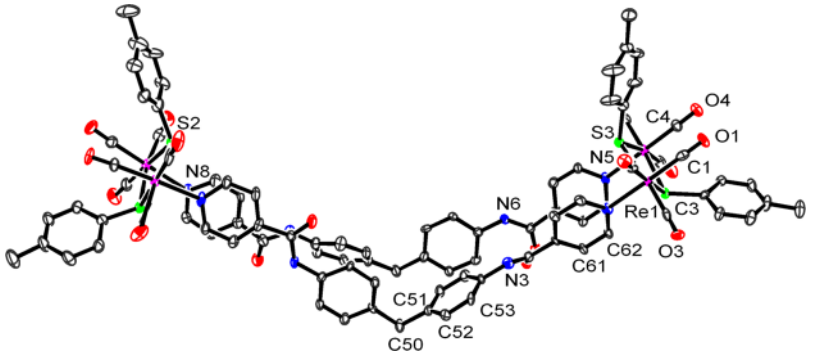

Figure 7. ORTEP diagram of $[\{(CO)_3Re(\mu\text{-}SC_6H_5CH_3)_2Re(CO)_3\}_2(\mu\text{-bpcpm})_2]$ (**7**•DMF) with thermal ellipsoids drawn at 40% probability level. Hydrogen atoms are omitted for clarity. Selected bond lengths (Å) and bond angles (°): Re(1)−N(4) 2.223(10), Re(1)−S(3) 2.522(3), Re(1)−S(4) 2.523(3), Re(1)−C(1) 1.936(13), Re(1)−C(2) 1.922(13), Re(1)−C(3) 1.921(16), N(4)−Re(1)−S(3) 82.6(3), N(4)−Re(1)−S(4) 86.2(2), Re(2)−S(3)−Re(1) 99.57(10), Re(2)−S(4)−Re(1) 99.59(10), S(3)−Re(1)−S(4) 79.34(10), and S(4)−Re(2)−S(3) 80.09(10).

EXPERIMENTAL SECTION

General Methods. All reactions were carried out under dry, oxygen-free N_2 atmosphere using standard Schlenk techniques. The starting materials were purchased from Sigma-Aldrich Chemicals. Rhenium carbonyl, dibutyldisulfide, dibenzyldisulfide, *p*-tolyldisulfide, and diphenyldiselenide were used as received. The bridging ligands *N*,*N*′-bis(4-pyridinecarboxamide)-1,2-ethane, *N*,*N*′-bis(4-(4-pyridylcarboxamide)phenyl)-methane, and diferrocenedisulfide were synthesized as reported in the literature.[17,7b] Mesitylene and other solvents were purified and dried using the literature procedure prior to use.[18] IR spectra were taken on a Thermo Nicolet iS10 Fourier transform infrared spectrometer. ^{1}H and ^{13}C NMR were recorded on an Avance Bruker 400 MHz spectrometer. Electronic absorption spectra were recorded on a Shimadzu UV-2450 UV−vis spectrophotometer. Emission spectra were recorded on a Fluoromax-4 spectrofluorometer. Elemental analyses were performed using a Thermo Scientific Flash 2000 CHNS analyzer. Compounds **1**−**8** were dried thoroughly under high vacuum condition for several hours, prior to the submission of samples for ^{1}H and ^{13}C NMR spectral characterization and elemental analyses.

Synthesis of $[\{(CO)_3Re(\mu\text{-}ER)_2Re(CO)_3\}_2(\mu\text{-}L)_2]$, General Procedure (1−8). A mixture of $Re_2(CO)_{10}$ (0.1 mmol), dialkyl/diaryl dichalcogenide (0.1 mmol), and ditopic amide-

DOI: 10.1021/acsomega.7b02075
ACS Omega 2018, 3, 3257−3266

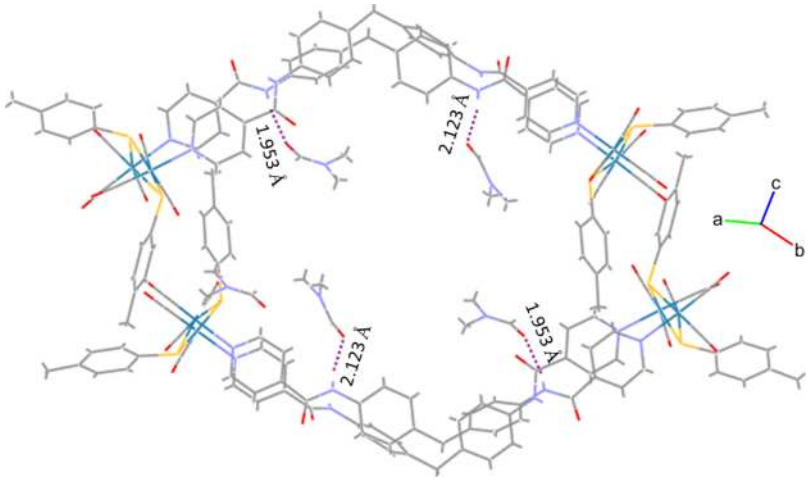

Figure 8. Packing diagram of **7** showing NH···OC hydrogen-bonding interactions between NH of metallacyclophane and carbonyl oxygen of DMF.

Table 1. Binding Constants (K_b) and Stern–Volmer Constants (K_{SV}) for Host–Guest Systems of 2 and 7 with Few Guests

	2		7	
guest	K_b, M^{-1}	K_{SV}, M^{-1}	K_b, M^{-1}	K_{SV}, M^{-1}
1,3,5-trimethoxy benzene	1.83×10^5	7.38×10^4	9.80×10^4	1.27×10^5
2,3,5-trimethoxy benzaldehyde	3.24×10^4	1.17×10^5	1.96×10^4	1.15×10^5
3,4,5-trimethoxy benzaldehyde	1.35×10^5	1.31×10^5	9.54×10^4	1.28×10^5

containing pyridyl ligand (L) (0.1 mmol) was taken in a Schlenk flask fitted with a reflux condenser. The system was evacuated and purged with N_2. To this, freshly distilled mesitylene (25 mL) was added and the reaction mixture was heated to 140 °C for 3 h. Color of the reaction mixture changed from white to yellow. The yellow compound was washed with hexane and subjected to chromatographic separation on a silica gel column. The product $[\{(CO)_3Re(\mu\text{-}ER)_2Re(CO)_3\}_2(\mu\text{-}L)_2]$ was isolated as a yellow solid and dried under vacuum.

Synthesis of $[\{(CO)_3Re(\mu\text{-}SC_4H_9)_2Re(CO)_3\}_2(\mu\text{-bpce})_2]$ (1). A mixture of $Re_2(CO)_{10}$ (65 mg, 0.1 mmol), dibutyldisulfide (31 mg, 0.1 mmol), and *N,N′*-bis(4-pyridinecarboxamide)-1,2-ethane (bpce) (27 mg, 0.1 mmol) in mesitylene (25 mL) was taken in a Schlenk flask fitted with a reflux condenser. The system was evacuated and purged with N_2. To this, freshly distilled mesitylene (25 mL) was added with positive pressure of nitrogen and the reaction mixture was heated to 140 °C for 3 h. Color of the reaction mixture changed from white to yellow yielding a yellow precipitate. The precipitate was washed with hexane and purified by silica gel column chromatography using a solvent mixture of hexane and acetone (4:1) as an eluent. The product $[\{(CO)_3Re(\mu\text{-}SC_4H_9)_2Re(CO)_3\}_2(\mu\text{-bpce})_2]$ (**1**) was isolated as a yellow solid and dried under vacuum. Yield: 41 mg, 44% [based on $Re_2(CO)_{10}$]. ^{1}H NMR (400 MHz, DMSO-d_6, ppm): δ 8.99 (d, 8H, H^2, py), 8.58 (s, 4H, NH), 7.72 (d, 8H, H^3, py), 3.68 (s, 8H, $NHCH_2$) 3.28 (t, 8H, H^1, Bu), 1.69 (m, 8H, H^2, Bu), 1.53 (m, 8H, H^3, Bu), 0.99 (t, 12H, H^4, Bu). ^{13}C NMR (100 MHz, DMSO-d_6, ppm): δ 200.9, 196.0 (1:2, CO), 164.9 (C═O), 156.6, 144.3, 123.8 (py), 40.4 (CH_2), 39.5, 35.8, 22.5, 14.1 (Bu). UV–vis (CH_2Cl_2) λ^{ab}_{max} (ε/dm^3 mol^{-1} cm^{-1}): 228 (19 240), 267 (12 182), 310 (7695), (LIG) 372 (3697) (MLCT). Anal. Calcd for $C_{56}H_{64}N_8O_{16}Re_4S_4$: C, 34.00; H, 3.26; N, 5.66; S, 6.48. Found: C, 33.82; H, 3.20; N, 5.58; S, 6.35. IR (CH_2Cl_2, cm^{-1}): ν 2021 (m), 2006 (s), 1919 (s), 1904 (s, ν_{CO}), 1663 (w, $\nu_{amide\ C=O}$).

Synthesis of $[\{(CO)_3Re(\mu\text{-}SCH_2C_6H_5)_2Re(CO)_3\}_2(\mu\text{-bpce})_2]$ (2). Compound **2** was prepared using $Re_2(CO)_{10}$ (65 mg, 0.1 mmol), dibenzyldisulfide (31 mg, 0.1 mmol), and *N,N′*-bis(4-pyridinecarboxamide)-1,2-ethane (bpce) (27 mg, 0.1 mmol) in mesitylene (25 mL) by following the procedure adopted for **1**. The product was isolated as a yellow solid of $[\{(CO)_3Re(\mu\text{-}SCH_2C_6H_5)_2Re(CO)_3\}_2(\mu\text{-bpce})_2]$ (**2**). Yield: 40 mg, 38% [based on $Re_2(CO)_{10}$]. ^{1}H NMR (400 MHz, acetone-d_6, ppm): δ 8.90 (d, 8H, H^2), 8.56 (s, 4H, NH), 7.69 (d, 8H, H^3, py), 7.55 (d, 8H, H^2, Bn), 7.35 (t, 8H, H^3, Bn), 7.29 (t, 12H, H^4, Bn), 4.46 (s, 8H, SCH_2, Bn), 3.67 (s, 8H, CH_2). ^{13}C NMR (100 MHz, acetone-d_6, ppm): δ 201.4 & 194.9 (1:2, CO), 164.8 (C═O), 156.5 (C^2, py), 144.3 (C^4, py), 142.5 (C^1, Ph), 129.7 (C^3, py), 129.5 (C^2, Ph), 128.1 (C^3, Ph), 123.7 (C^4, Ph), 43.6 (SCH_2, Bn), 40.6 (CH_2). UV–vis (CH_2Cl_2) λ^{ab}_{max} (ε/dm^3 mol^{-1} cm^{-1}): 229 (23 727), 267 (13 650), 311 (10 502) (LIG), 369 (2750) (MLCT). Anal. Calcd for $C_{68}H_{56}N_8O_{16}Re_4S_4$: C, 38.63; H, 2.67; N, 5.32; S, 6.07. Found C, 38.82; H, 2.59; N, 5.32; S, 5.99. IR (CH_2Cl_2, cm^{-1}) ν 2021 (m), 2007 (s), 1919 (s), 1907 (s, ν_{CO}), 1660 (w, $\nu_{amide\ C=O}$).

Synthesis of $[\{(CO)_3Re(\mu\text{-}SC_4H_5FeC_5H_5)_2Re(CO)_3\}_2(\mu\text{-bpce})_2]$ (3). Compound **3** was prepared using $Re_2(CO)_{10}$ (65 mg, 0.1 mmol), diferrocenedisulfide (45 mg, 0.1 mmol), and *N,N′*-bis(4-pyridinecarboxamide)-1,2-ethane (bpce) (27 mg, 0.1 mmol) in mesitylene (25 mL) by following the procedure adopted for **1**. The product was isolated as a yellow solid of $[\{(CO)_3Re(\mu\text{-}SC_5H_4FeC_5H_5)_2Re(CO)_3\}_2(\mu\text{-bpce})_2]$ (**3**). Yield: 45 mg, 37% [based on $Re_2(CO)_{10}$]. ^{1}H NMR (400 MHz, DMSO-d_6, ppm): δ 9.05 (s, 4H, NH), 9.03 (d, 8H, H^2, py), 7.82 (d, 8H, H^3, py), 4.54 (m, 8H, H^2, C_5H_4), 4.27 (m, 8H, H^3, C_5H_4), 4.22 (s, 20H, 8H, C_5H_5), 3.53 (s, 8H, CH_2). UV–vis (CH_2Cl_2) λ^{ab}_{max} (ε/dm^3 mol^{-1} cm^{-1}): 229 (39 922), 270 (17 802), 310 (10 590) (LIG), 383 (3757) (MLCT). Anal. Calcd for $C_{80}H_{64}N_8O_{16}S_4Fe_4Re_4$: C, 38.59; H, 2.59; N, 4.50; S, 5.15. Found C, 38.30; H, 2.65; N, 4.34; S, 5.08. IR (CH_2Cl_2,

DOI: 10.1021/acsomega.7b02075
ACS Omega 2018, 3, 3257–3266

cm^{-1}): ν 2027 (m), 2012 (s), 1926 (s), 1902 (s, ν_{CO}), 1605 (w, $\nu_{amide\ C=O}$).

Synthesis of [{(CO)$_3$Re(μ-SeC$_6$H$_5$)$_2$Re(CO)$_3$}$_2$(μ-bpce)$_2$] (4). Compound **4** was prepared using $Re_2(CO)_{10}$ (65 mg, 0.1 mmol), diphenyldiselenide (31 mg, 0.1 mmol), and *N*,*N*′-bis(4-pyridinecarboxamide)-1,2-ethane (bpce) (27 mg, 0.1 mmol) in mesitylene (25 mL) by following the procedure adopted for **1**. The product was isolated as a yellow solid of [{(CO)$_3$Re(μ-SeC$_6$H$_5$)$_2$Re(CO)$_3$}$_2$(μ-bpce)$_2$] (**4**). Yield: 42 mg, 40% [based on $Re_2(CO)_{10}$]. ^{1}H NMR (400 MHz, acetone-d_6, ppm): δ 9.28 (d, 8H, H^2, py), 8.70 (s, 4H, NH), 7.87 (m, 16H, py & Ph), 7.34 (t, 8H, H^3, Ph), 7.26 (t, 4H, H^4, Ph), 3.77 (t, 8H, CH_2). ^{13}C NMR (100 MHz, acetone-d_6, ppm): δ 200.2, 194.7 (1:2, CO), 164.1 (C=O), 157.9 (C^2, py), 144.7 (C^4, py), 133.8 (C^1, Ph), 131.3 (C^3, py), 129.6 (C^2, Ph), 127.3 (C^3, Ph), 124.3 (C^4, Ph), 40.6 (CH_2). UV−vis (CH_2Cl_2) λ^{ab}_{max} (ε/dm^3 mol^{-1} cm^{-1}): 235 (27 362), 268 (20 245), 311 (10 957) (LIG), 380 (4542) (MLCT). Anal. Calcd for $C_{64}H_{48}N_8O_{16}Re_4Se_4$: C, 34.23; H, 2.15; N, 4.99. Found C, 34.13; H, 2.18; N, 4.51. IR (CH_2Cl_2, cm^{-1}): ν 2029 (s), 2014 (s), 1932 (s), 1904 (s, ν_{CO}), 1663 (w, $\nu_{amide\ C=O}$).

Synthesis of [{(CO)$_3$Re(μ-SC$_4$H$_9$)$_2$Re(CO)$_3$}$_2$(μ-bpcpm)$_2$] (5). Compound **5** was prepared using $Re_2(CO)_{10}$ (65 mg, 0.1 mmol), dibutyldisulfide (31.2 mg, 0.1 mmol), and *N*,*N*′-bis(4-(4-pyridylcarboxamide)phenyl)methane (bpcpm) in mesitylene (25 mL) by following the procedure adopted for **1**. The product was isolated as a yellow solid of [{(CO)$_3$Re(μ-SC$_4$H$_9$)$_2$Re(CO)$_3$(μ-bpcpm)$_2$] (**5**). Yield: 62 mg, 44% [based on $Re_2(CO)_{10}$]. ^{1}H NMR (400 MHz, acetone-d_6, ppm): δ 9.75 (s, 4H, NH), 9.04 (d, 8H, H^2, py), 7.76 (d, 8H, H^3, py), 7.68 (d, 8H, H^2, Ph), 7.19 (d, 8H, H^2, Ph), 4.06 (s, 4H, CH_2), 3.28 (t, 8H, H^1, Bu), 1.70 (m, 8H, H^2, Bu), 1.55 (m, 8H, H^2, Bu), 1.00 (t, 12H, H^4, Bu). ^{13}C NMR (100 MHz, acetone-d_6, ppm): δ 201.1, 196.1 (1:2, CO), 163.2 (C=O), 156.5 (C^2, py), 145.1 (C^4, py), 138.5 (C^1, Ph), 137.3 (C^4, Ph), 129.9 (C^3, py), 123.9 (C^2, Ph), 122.0 (C^3, Ph), 41.3 (CH_2), 39.6, 35.7, 22.4, 14.0 (Bu). UV−vis (CH_2Cl_2) λ^{ab}_{max} (ε/dm^3 mol^{-1} cm^{-1}): 232 (46 802), 274 (20 959) (LIG), 312 (21 183) (MLCT). Anal. Calcd for $C_{78}H_{72}N_8O_{16}Re_4S_4$: C, 41.55; H, 3.40; N, 4.97; S, 5.69. Found C, 41.09; H, 3.45; N, 5.01; S, 5.63. IR (CH_2Cl_2, cm^{-1}): ν 2020 (s), 2003 (s), 1918 (m), 1897 (s, ν_{CO}), 1606 (w, $\nu_{amide\ C=O}$).

Synthesis of [{(CO)$_3$Re(μ-SCH$_2$C$_6$H$_5$)$_2$Re(CO)$_3$}$_2$(μ-bpcpm)$_2$] (6). Compound **6** was prepared using $Re_2(CO)_{10}$ (65 mg, 0.1 mmol), dibenzyldisulfide (31 mg, 0.1 mmol), and *N*,*N*′-bis(4-(4-pyridylcarboxamide)phenyl)methane (bpcpm) in mesitylene (25 mL) by following the procedure adopted for **1**. The product was isolated as a yellow solid of [{(CO)$_3$Re(μ-SCH$_2$C$_6$H$_5$)$_2$Re(CO)$_3$}$_2$(μ-bpcpm)$_2$] (**6**). Yield: 66 mg, 47% [based on $Re_2(CO)_{10}$]. ^{1}H NMR (400 MHz, acetone-d_6, ppm): δ 9.84 (s, 4H, NH), 8.93 (d, 8H, H^2, py), 7.71 (d, 8H, H^3, py), 7.66 (d, 8H, H^2, Bn), 7.57 (d, 8H, H^2, Bn), 7.35 (t, 8H, H^3, Bn), 7.28 (t, 4H, H^4, Bn), 7.19 (d, 8H, H^3, Ph), 4.45 (s, 8H, CH_2, Bn), 4.06 (s, 4H, CH_2). ^{13}C NMR (100 MHz, acetone-d_6, ppm): δ 202.0, 194.9 (1:2, CO), 163.1 (C=O), 156.5 (C^2, py), 145.0 (C^4, py), 142.4 (C^1, Ph, Bn), 138.5 (C^1, Ph), 137.4 (C^4, Ph), 129.9 (C^3, py), 129.7 (C^2, Ph, Bn), 129.5 (C^2, Ph), 128.0 (C^3, Ph, Bn), 123.9 (C^4, Ph, Bn), 122.0 (C^3, Ph), 43.5 (CH_2, Bn), 41.3 (CH_2). UV−vis (CH_2Cl_2) λ^{ab}_{max} (ε/dm^3 mol^{-1} cm^{-1}): 226 (19 534), 274 (9746) (LIG), 327 (5836) (MLCT). Anal. Calcd for $C_{90}H_{68}N_8O_{16}Re_4S_4$: C, 45.22; H, 2.87; N, 4.69; S, 5.37. Found C, 45.30; H, 2.85; N, 4.70; S, 5.31. IR (CH_2Cl_2, cm^{-1}): ν 2021 (s), 2006 (s), 1917 (m), 1906 (s. ν_{CO}), 1681 (w, $\nu_{amide\ C=O}$).

Synthesis of [{(CO)$_3$Re(μ-SC$_6$H$_5$CH$_3$)$_2$Re(CO)$_3$}$_2$(μ-bpcpm)$_2$] (7). Compound **7** was prepared using $Re_2(CO)_{10}$ (65 mg, 0.1 mmol), *p*-tolyldisulfide (31 mg, 0.1 mmol), and *N*,*N*′-bis(4-(4-pyridylcarboxamide)phenyl)methane (bpcpm) in mesitylene (25 mL) by following the procedure adopted for **1**. The product was isolated as a yellow solid of [{(CO)$_3$Re(μ-SC$_6$H$_5$CH$_3$)$_2$Re(CO)$_3$}$_2$(μ-bpcpm)$_2$] (**7**). Yield: 86 mg, 52% [based on $Re_2(CO)_{10}$]. ^{1}H NMR (400 MHz, acetone-d_6, ppm): δ 9.84 (s, 4H, NH), 9.22 (d, 8H, H^2, py), 7.85 (d, 8H, H^3, py), 7.76 (d, 8H, H^2, Ph), 7.71 (d, 8H, H^2, *p*-tolyl), 7.21 (m, 16H, H^3, *p*-tolyl & H^3, Ph), 4.07 (s, 4H, CH_2), 2.35 (s, 12H, CH_3, *p*-tolyl). ^{13}C NMR (100 MHz, acetone-d_6, ppm): δ 200.5, 196.4 (1:2, CO), 163.4 (C=O), 156.9 (C^2, py), 145.5 (C^4, py), 138.7 (C^1, Ph, *p*-tolyl), 137.4 (C^1, Ph), 136.6 (C^4, Ph), 132.3 (C^3, py), 130.0 (C^2, Ph, *p*-tolyl), 129.9 (C^2, Ph), 127.6 (C^3, Ph, *p*-tolyl), 124.0 (C^4, Ph, *p*-tolyl), 122.1 (C^3, Ph) 21.4 (CH_3), 41.2 (CH_2). UV−vis (CH_2Cl_2) λ^{ab}_{max} (ε/dm^3 mol^{-1} cm^{-1}): 229 (33 842), 269 (19 297) (LIG), 305 (14 027) (MLCT). Anal. Calcd for $C_{90}H_{68}N_8O_{16}Re_4S_4$: C, 45.22; H, 2.87; N, 4.69; S, 5.37. Found C, 45.20; H, 2.82; N, 4.67; S, 5.34. IR (CH_2Cl_2, cm^{-1}): ν 2028 (s), 2013 (s), 1929 (m), 1906 (s, ν_{CO}), 1641 (w, $\nu_{amide\ C=O}$).

Synthesis of [{(CO)$_3$Re(μ-SeC$_6$H$_5$)$_2$Re(CO)$_3$}$_2$(μ-bpcpm)$_2$] (8). Compound **8** was prepared using $Re_2(CO)_{10}$ (65 mg, 0.1 mmol), *p*-tolyldisulfide (31 mg, 0.1 mmol), and *N*,*N*′-bis(4-(4-pyridylcarboxamide)phenyl)methane (bpcpm) in mesitylene (25 mL) by following the procedure adopted for **1**. The product was isolated as a yellow solid of [{(CO)$_3$Re(μ-SeC$_6$H$_5$)$_2$Re(CO)$_3$}$_2$(μ-bpcpm)$_2$] (**8**). Yield: 72 mg, 41% [based on $Re_2(CO)_{10}$]. ^{1}H NMR (400 MHz, acetone-d_6, ppm): δ 9.92 (s, 4H, NH), 9.32 (d, 8H, H^2, py), 7.91 (m, 16H, H^3, py & H^2, SePh), 7.74 (d, 8H, H^3, Ph), 7.35 (t, 8H, H^3, SePh), 7.26 (t, 4H, H^4, SePh), 7.21 (d, 8H, H^3, Ph), 4.07 (s, 4H, CH_2). ^{13}C NMR (100 MHz, acetone-d_6, ppm): δ 199.9, 194.9 (1:2, CO), 163.3 (C=O), 157.9 (C^2, py), 145.6 (C^4, py), 138.7 (C^1, SePh), 137.4 (C^1, Ph), 133.8 (C^4, Ph), 131.4 (C^3, py), 130.0 (C^2, SePh), 129.7 (C^2, Ph), 127.6 (C^3, SePh), 127.3 (C^4, SePh), 124.5 (C^3, SePh), 122.1 (C^3, Ph) 41.39 (CH_2). UV−vis (CH_2Cl_2) λ^{ab}_{max} (ε/dm^3 mol^{-1} cm^{-1}): 227 (8461), 269 (4340) (LIG), 307 (3591) (MLCT). Anal. Calcd for $C_{86}H_{60}N_8O_{16}R,e_4Se_4$: C 40.95; H, 2.40; N, 4.44. Found C, 39.55; H, 2.36; N, 4.51. IR (CH_2Cl_2, cm^{-1}): ν 2028 (s), 2013 (s), 1931 (m), 1903 (s, ν_{CO}), 1663 (w, $\nu_{amide\ C=O}$).

Single-Crystal X-ray Diffraction Studies. Good-quality crystals of **1**−**3** and **7** suitable for the single-crystal X-ray structure analysis were grown by slow evaporation of concentrated solution of compound in DMF and dichloroethane at 5 °C. Single-crystal X-ray structural studies were performed on a CCD Oxford Diffraction XCALIBUR-S diffractometer equipped with an Oxford Instruments low-temperature attachment. Crystal data were collected using graphite-monochromated Mo Kα radiation (λ_α = 0.71073 Å). The strategy for the data collection was evaluated by using the CrysAlisPro CCD software. The data were collected by the standard 'ψ−ω scan' techniques and were scaled and reduced using CrysAlisPro RED software. The structures were solved by direct methods (SHELXS) and refined by full-matrix leastsquares calculations on F^2 (SHELXL).[19] A dichloroethane molecule present in the crystal lattice of **2** was squeezed with the Squeeze algorithm, and the structure was refined to convergence.[20] The positions on all the atoms were obtained by

DOI: 10.1021/acsomega.7b02075
ACS Omega 2018, 3, 3257−3266

direct methods. All nonhydrogen atoms were refined anisotropically. The hydrogen atoms were placed in geometrically constrained positions and refined with isotropic temperature factors, generally 1.2 × U_{eq} of their parent atoms.

■ ASSOCIATED CONTENT

Supporting Information

The Supporting Information is available free of charge on the ACS Publications website at DOI: 10.1021/acsomega.7b02075.

Crystallographic data and structure refinement details of **1**−**3** and **7**, experimental procedures for molecular recognition studies, overlay electronic absorption, and emission spectra, Benesi−Hildebrand linear regression plots and Stern−Volmer plots of **2** and **7** with guest molecules, and ^{1}H NMR spectral titration experiments of **2** and **6** with 2,4,5-trimethoxybenzaldehyde (PDF)

Crystallographic data for **1**·DMF, **2**, **2**·DMF, **3** and **7**·DMF (CIF)

■ AUTHOR INFORMATION

Corresponding Author

*E-mail: manimaran.che@pondiuni.edu.in (B.M.).

ORCID

Buthanapalli Ramakrishna: 0000-0002-8967-6167

Notes

The authors declare no competing financial interest.

■ ACKNOWLEDGMENTS

We thank the Department of Science and Technology, Government of India and Council of Scientific and Industrial Research, Government of India for financial support. M.K. and B.R.K. acknowledge UGC Government of India for financial assistance. D.D. gratefully acknowledges CSIR Government of India for the award of Senior Research Fellowship. We are grateful to the Central Instrumentation Facility, Pondicherry University for providing spectral data. We are thankful to the DST-FIST program sponsored Single-crystal X-ray diffraction facility to the Department of Chemistry, Pondicherry University.

■ REFERENCES

(1) (a) DeFlores, L. P.; Ganim, Z.; Nicodemus, R. A.; Tokmakoff, A. Amide I′-II′ 2D IR Spectroscopy Provides Enhanced Protein Secondary Structural Sensitivity. *J. Am. Chem. Soc.* **2009**, *131*, 3385−3391. (b) Zhao, J.; Wang, J. Amide Vibrations and Their Conformational Dependences in *β*-Peptide. *J. Phys. Chem. B* **2010**, *114*, 16011−16019. (c) Ye, S.; Li, H.; Yang, W.; Luo, Y. Accurate Determination of Interfacial Protein Secondary Structure by Combining Interfacial-Sensitive Amide I and Amide III Spectral Signals. *J. Am. Chem. Soc.* **2014**, *136*, 1206−1209. (d) Zhang, Y. P.; Lewis, R. N. A. H.; Hodges, R. S.; McElhaney, R. N. FTIR Spectroscopic Studies of the Conformation and Amide Hydrogen Exchange of a Peptide Model of the Hydrophobic Transmembrane-Helices of Membrane Proteins. *Biochemistry* **1992**, *31*, 11572−11578.

(2) (a) Maekawa, H.; Ballano, G.; Toniolo, C.; Ge, N.-H. Linear and Two-Dimensional Infrared Spectroscopic Study of the Amide I and II Modes in Fully Extended Peptide Chains. *J. Phys. Chem. B* **2010**, *115*, 5168−5182. (b) Overman, S. A.; Thomas, G. J. Amide Modes of the *α*-Helix: Raman Spectroscopy of Filamentous Virus *fd* Containing Peptide ^{13}C and ^{2}H Labels in Coat Protein Subunits. *Biochemistry* **1998**, *37*, 5654−5665. (c) Leoncini, A.; Ansari, S. A.; Mohapatra, P. K.; Boda, A.; Ali, S. M.; Sengupta, A.; Huskens, J.; Verboom, W. Benzene-centered tripodal diglycolamides: synthesis, metal ion extraction, luminescence spectroscopy, and DFT studies. *Dalton Trans.* **2017**, *46*, 1431−1438.

(3) (a) Zabicky, J. *The Chemistry of Amides*; Wiley-Interscience: New York, 1970. (b) Greenberg, A.; Breneman, C. M.; Liebman, John J. F. The Amide Linkages: Structural Significance in Chemistry. *Biochemistry and Material Science*; Wiley & Sons: New York, 2000.

(4) (a) Eberhardt, E. S.; Raines, R. T. Amide-Amide and Amide-Water Hydrogen Bonds: Implications for Protein Folding and Stability. *J. Am. Chem. Soc.* **1994**, *116*, 2149−2150. (b) Zhai, X.; Brezesinski, G.; Möhwald, H.; Li, J. Thermodynamics and Structures of Amide Phospholipid Monolayers. *J. Phys. Chem. B* **2004**, *108*, 13475−13480. (c) Paul-Roth, C.; Raymond, K. N. Amide Functional Group Contribution to the Stability of Gadolinium(III) Complexes: DTPA Derivatives. *Inorg. Chem.* **1995**, *34*, 1408−1412. (d) Yang, L.; Houser, R. P. Copper(I) Coordination Chemistry of (Pyridylmethyl)-amide Ligands. *Inorg. Chem.* **2006**, *45*, 9416−9422. (e) Clapp, L. A.; Siddons, C. J.; Whitehead, J. R.; VanDerveer, D. G.; Rogers, R. D.; Griffin, S. T.; Jones, S. B.; Hancock, R. D. Factors Controlling Metal-Ion Selectivity in the Binding Sites of Calcium-Binding Proteins. The Metal-Binding Properties of Amide Donors. A Crystallographic and Thermodynamic Study. *Inorg. Chem.* **2005**, *44*, 8495−8502. (f) Onoda, A.; Yamada, Y.; Okamura, T. A.; Yamamoto, H.; Ueyama, N. Mononuclear Ca(II)-Bulky Aryl-Phosphate Monoanion and Dianion Complexes with Ortho-Amide Groups. *Inorg. Chem.* **2002**, *41*, 6038−6047. (g) Sigel, H.; Martin, R. B. Coordinating Properties of the Amide Bond. Stability and Structure of Metal Ion Complexes of Peptides and Related Ligands. *Chem. Rev.* **1982**, *82*, 385−426.

(5) (a) Hartgerink, J. D.; Clark, T. D.; Ghadiri, M. R. Peptide Nanotubes and Beyond. *Chem.—Eur. J.* **1998**, *4*, 1367−1372. (b) Ghadiri, M. R.; Kobayashi, K.; Granja, J. R.; Chadha, R. K.; Mcree, D. E. The Structural and Thermodynamic Basis for the Formation of Self-Assembled Peptide Nanotubes. *Angew. Chem., Int. Ed.* **1995**, *34*, 93−95. (c) Huang, K.; Xu, Z.; Li, Y.; Zheng, H. Guest-Induced Helical Metallacyclic Chains in a Porous Coordination Solid Constructed from a Flexible Ester-Containing Ligand. *Cryst. Growth Des.* **2007**, *7*, 202−204. (d) Lawrence, D. S.; Jiang, T.; Levett, M. Self-Assembling Supramolecular Complexes. *Chem. Rev.* **1995**, *95*, 2229−2260. (e) Ghosh, T. K.; Chakraborty, S.; Chowdhury, B.; Ghosh, P. Bis-Heteroleptic Ruthenium(II) Complex of Pendant Urea Functionalized Pyridyl Triazole and Phenathroline for Recognition, Sensing, and Extraction of Oxyanions. *Inorg. Chem.* **2017**, *56*, 5371−5382.

(6) (a) Shanmugaraju, S.; Bar, A. K.; Chi, K. W.; Mukherjee, P. S. Coordination-Driven Self-Assembly of Metallamacrocycles via a New Pt^{II}_{2} Organometallic Building Block with 90° Geometry and Optical Sensing of Anions. *Organometallics* **2010**, *29*, 2971−2980. (b) Jones, C. D.; Tan, J. C.; Lloyd, G. O. Supramolecular Isomerism of a Metallocyclic Dipyridyl Diamide Ligand Metal Halide System Generating Isostructural (Hg, Co And Zn) Porous Materials. *Chem. Commun.* **2012**, *48*, 2110−2112. (c) Sadhukhan, N.; Sinha, A.; Das, R. K.; Bera, J. K. Multi-site Coordination of Ferrocenyl Amido-Naphthyridine Conjugates [{(5,7-dimethyl-1,8-naphthyridin-2-yl)-amino}carbonyl]ferrocene and 1,10-bis[{(5,7-dimethyl-1,8-naphthyridin-2-yl)amino}carbonyl]ferrocene. *J. Organomet. Chem.* **2010**, *695*, 67−73. (d) Huynh, H. V.; Schulze-Isfort, C.; Seidel, W. W.; Lügger, T.; Fröhlich, R.; Kataeva, O.; Hahn, F. E. Dinuclear Complexes with Bis(benzenedithiolate) Ligands. *Chem.—Eur. J.* **2002**, *8*, 1327−1335. (e) Shanmugaraju, S.; Joshi, S. A.; Mukherjee, P. S. Self-Assembly of Metallamacrocycles Using a Dinuclear Organometallic Acceptor: Synthesis, Characterization, and Sensing Study. *Inorg. Chem.* **2011**, *50*, 11736−11745.

(7) (a) Ghosh, S.; Mukherjee, P. S. Self-assembly of Metal−Organic Hybrid Nanoscopic Rectangles. *Dalton Trans.* **2007**, 2542−2546. (b) Shanmugaraju, S.; Bar, A. K.; Joshi, S. A.; Patil, Y. P.; Mukherjee, P. S. Constructions of 2D-Metallamacrocycles Using Half-Sandwich $RuII_{2}$ Precursors: Synthesis, Molecular Structures, and Self-Selection for a Single Linkage Isomer. *Organometallics* **2011**, *30*, 1951−1960. (c) Mishra, A.; Jung, H.; Park, J. W.; Kim, H. K.; Kim, H.; Stang, P. J.; Chi, K.-W. Anticancer Activity of Self-Assembled Molecular Rectangles

DOI: 10.1021/acsomega.7b02075
ACS Omega 2018, 3, 3257−3266

via Arene−Ruthenium Acceptors and a New Unsymmetrical Amide Ligand. *Organometallics* **2012**, *31*, 3519−3526. (d) Vivekananda, K. V.; Dey, S.; Maity, D. K.; Bhuvanesh, N.; Jain, V. K. Supramolecular Macrocyclic Pd(II) and Pt(II) Squares and Rectangles with Aryl dithiolate Ligands and their Excellent Catalytic Activity in Suzuki C−C Coupling Reaction. *Inorg. Chem.* **2015**, *54*, 10153−10162. (e) Ashok Kumar, C.; Nagarajaprakash, R.; Ramakrishna, B.; Manimaran, B. Self-assembly of Thiolato-Bridged Manganese(I)-Based Metallarectangles: One-pot Synthesis and Structural Characterization. *Inorg. Chem.* **2015**, *54*, 8406−8414. (f) Govindarajan, R.; Nagarajaprakash, R.; Manimaran, B. Synthesis, Structural Characterization, and Host−Guest Studies of Aminoquinonato-Bridged Re(I) Supramolecular Rectangles. *Inorg. Chem.* **2015**, *54*, 10686−10694. (g) Nagarajaprakash, R.; Divya, D.; Ramakrishna, B.; Manimaran, B. Synthesis and Spectroscopic and Structural Characterization of Oxamidato-Bridged Rhenium(I) Supramolecular Rectangles with Ester Functionalization. *Organometallics* **2014**, *33*, 1367−1373. (h) Rajakannu, P.; Hussain, F.; Shankar, B.; Sathiyendiran, M. Unprecedented single-crystal-to-single-crystal topochemical conformational change and photoreduction of ethylene units in π-stacked metallomacrocycle. *Inorg. Chem. Commun.* **2012**, *26*, 46−50. (i) He, Z.; Li, M.; Que, W.; Stang, P. J. Self-Assembly of Metal-Ion-Responsive Supramolecular Coordination Complexes and their Photophysical Properties. *Dalton Trans.* **2017**, *46*, 3120−3124.

(8) (a) Vajpayee, V.; Song, Y. H.; Lee, M. H.; Kim, H.; Wang, M.; Stang, P. J.; Chi, K. W. Self-Assembled Arene−Ruthenium-Based Rectangles for the Selective Sensing of Multi-Carboxylate Anions. *Chem.—Eur. J.* **2011**, *17*, 7837−7844. (b) Mishra, A.; Jung, H.; Lee, M. H.; Lah, M. S.; Chi, K.-W. Synthesis and Characterization of Self-Assembled Nanoscopic Metallarectangles Capable of Binding Fullerenes with Size-Selective Responses. *Inorg. Chem.* **2013**, *52*, 8573−8578. (c) Shanmugaraju, S.; Vajpayee, V.; Lee, S.; Chi, K.-W.; Stang, P. J.; Mukherjee, P. S. Coordination-Driven Self-Assembly of 2D-Metallamacrocycles Using a New Carbazole-Based Dipyridyl Donor: Synthesis, Characterization, and C_{60} Binding Study. *Inorg. Chem.* **2012**, *51*, 4817−4823. (d) Dubey, A.; Jeong, Y. J.; Jo, J. H.; Woo, S.; Kim, D. H.; Kim, H.; Kang, S. C.; Stang, P. J.; Chi, K.-W. Anticancer Activity and Autophagy Involvement of Self-Assembled Arene−Ruthenium Metallacycles. *Organometallics* **2015**, *34*, 4507−4514. (e) Roy, B.; Saha, R.; Ghosh, A. K.; Patil, Y.; Mukherjee, P. S. Versatility of Two Diimidazole Building Blocks in Coordination-Driven Self-Assembly. *Inorg. Chem.* **2017**, *56*, 3579−3588.

(9) (a) Mishra, A.; Vajpayee, V.; Kim, H.; Lee, M. H.; Jung, H.; Wang, M.; Stang, P. J.; Chi, K.-W. Self-Assembled Metalla-Bowls for Selective Sensing of Multi-Carboxylate Anions. *Dalton Trans.* **2012**, *41*, 1195−1201. (b) Mishra, A.; Ravikumar, S.; Song, Y. H.; Prabhu, N. S.; Kim, H.; Hong, S. H.; Cheon, S.; Noh, J.; Chi, K.-W. A New Arene−Ru Based Supramolecular Coordination Complex for Efficient Binding and Selective Sensing of Green Fluorescent Protein. *Dalton Trans.* **2014**, *43*, 6032−6040.

(10) (a) Gancheff, J. S.; Albuquerque, R. Q.; Guerrero-Martinez, A.; Pape, T.; Cola, L. D.; Hahn, F. E. A Dinuclear Double-Stranded Oxido Complex of ReV with a Bis(benzene-*o*-dithiolato) Ligand. *Eur. J. Inorg. Chem.* **2009**, 4043−4051. (b) Tzeng, B.-C.; Chen, Y.-F.; Wu, C.-C.; Hu, C.-C.; Chang, Y.-T.; Chen, C.-K. Anion-Recognition Studies of a Re(I)-Based Square Containing the Dipyridyl-Amide Ligand. *New J. Chem.* **2007**, *31*, 202−209. (c) Nagarajaprakash, R.; Govindarajan, R.; Manimaran, B. One-Pot Synthesis of Oxamidato-Bridged Hexarhenium Trigonal Prisms Adorned with Ester Functionality. *Dalton Trans.* **2015**, *44*, 11732−11740. (d) Ramakrishna, B.; Nagarajaprakash, R.; Veena, V.; Sakthivel, N.; Manimaran, B. Self-Assembly of Oxamidato Bridged Ester Functionalised Dirhenium Metallastirrups: Synthesis, Characterisation and Cytotoxicity Studies. *Dalton Trans.* **2015**, *44*, 17629−17638. (e) Ramakrishna, B.; Ashok Kumar, C.; Logesh, T. J.; Manimaran, B. Oxamidato Pillared Heteroligated Dirhenium(I) Metallacrown Ethers: Synthesis, Spectroscopic and Structural Characterization. *J. Organomet. Chem.* **2017**, *828*, 116−121. (f) Ashok Kumar, C.; Divya, D.; Nagarajaprakash, R.; Veena, V.; Vidhyapriya, P.; Sakthivel, N.; Manimaran, B. Self-Assembly of Manganese(I) and Rhenium(I) Based Semi-Rigid Ester Functionalized M_2L_2-Type Metallacyclophanes Synthesis, Characterization and Cytotoxicity Evaluation. *J. Organomet. Chem.* **2017**, *846*, 152−160.

(11) (a) Manimaran, B.; Thanasekaran, P.; Rajendran, T.; Lin, R. J.; Chang, J. I.; Lee, G. H.; Peng, S. M.; Rajagopal, S.; Lu, K. L. Luminescence Enhancement Induced by Aggregation of Alkoxy-Bridged Rhenium(I) Molecular Rectangles. *Inorg. Chem.* **2002**, *41*, 5323−5325. (b) Benkstein, K. D.; Hupp, J. T.; Stern, C. L. Synthesis and Characterization of Molecular Rectangles Based upon Rhenium Thiolate Dimers. *Inorg. Chem.* **1998**, *37*, 5404−5405. (c) Ramakrishna, B.; Divya, D.; Monisha, P. V.; Manimaran, B. Self-Assembly of Oxamidato-Chelated Re^{I}- and Mn^{I}-Based Flexible Dinuclear Horse-Stirrup-Like Metallacycles. *Eur. J. Inorg. Chem.* **2015**, 5839−5846.

(12) Rajendran, T.; Manimaran, B.; Liao, R.-T.; Lin, R.-J.; Thanasekaran, P.; Lee, G.-H.; Peng, S.-M.; Liu, Y.-H.; Chang, I.-J.; Rajagopal, S.; Lu, K.-L. Synthesis and Photophysical Properties of Neutral Luminescent Rhenium-Based Molecular Rectangles. *Inorg. Chem.* **2003**, *42*, 6388−6394.

(13) Burchell, T. J.; Eisler, D. J.; Puddephatt, R. J. Self-Assembly Using Dynamic Coordination Chemistry and Hydrogen Bonding: Mercury(II) Macrocycles, Polymers and Sheets. *Inorg. Chem.* **2004**, *43*, 5550−5557.

(14) (a) Manimaran, B.; Lai, L.-J.; Thanasekaran, P.; Wu, J.-Y.; Liao, R.-T.; Tseng, T.-W.; Liu, Y.-H.; Lee, G.-H.; Peng, S.-M.; Lu, K.-L. CH●●●π Interaction for Rhenium-Based Rectangles: An Interaction that is Rarely Designed into a Host-Guest Pair. *Inorg. Chem.* **2006**, *45*, 8070−8077. (b) Manimaran, B.; Vanitha, A.; Karthikeyan, M.; Ramakrishna, B.; Mobin, S. M. Self-Assembly of Selenium-Bridged Rhenium(I)-Based Metalla Rectangles: Synthesis, Characterization, and Molecular Recognition Studies. *Organometallics* **2014**, *33*, 465−472.

(15) Hunter, C. A.; Sanders, J. K. M. The Nature of π-π Interactions. *J. Am. Chem. Soc.* **1990**, *112*, 5525−5534.

(16) (a) Benesi, H. A.; Hildebrand, J. H. Spectrophotometric Investigation of the Interaction of Iodine with Aromatic Hydrocarbons. *J. Am. Chem. Soc.* **1949**, *71*, 2703−2707. (b) Manimaran, B.; Thanasekaran, P.; Rajendran, T.; Liao, R.-T.; Liu, Y.-H.; Lee, G.-H.; Peng, S.-M.; Rajagopal, S.; Lu, K.-L. Self-Assembly of Octarhenium-Based Neutral Luminescent Rectangular Prisms. *Inorg. Chem.* **2003**, *42*, 4795−4797.

(17) Stern, O.; Volmer. The Fading Time of Fluorescence. M. *Phys. Z.* **1919**, *20*, 183−188.

(18) Armarego, W. L. F.; Chai, C. L. L. *Purification of Laboratory Chemicals*, 6th ed.; Butterworth-Heinemann, Elsevier Inc.: Oxford, 2009.

(19) (a) Sheldrick, G. M. Short History of SHELX. *Acta Crystallogr., Sect. A: Found. Crystallogr.* **2008**, *64*, 112−122. (b) Sheldrick, G. M. Crystal Structure Refinement with SHELXL. *Acta Crystallogr. Sect. C: Fundam. Crystallogr.* **2015**, *71*, 3−8. (c) Farrugia, L. J. ORTEP-3 for Windows - a version of ORTEP-III with a Graphical User Interface (GUI). *J. Appl. Crystallogr.* **1997**, *30*, 565.

(20) Spek, A. L.; PLATON, A. *Multipurpose Crystallographic Tool*; Utrecht University: Utrecht, The Netherlands, 2008.

DOI: 10.1021/acsomega.7b02075
ACS Omega 2018, 3, 3257−3266